Fluorescent responses of CdSe and Si QDs toward Copper (II) ion and the mixed-QDs probe for Cu^{2+} ion sensing

Authors: Nattakarn Phromsiri[a], Sakiru L. Abiodun[b], Chonnavee Manipuntee[a], Pannee Leeladee[a], Andrew B. Greytak[b], Numpon Insin[*a].

[a] department of Chemistry, Faculty of Science, Chulalongkorn University, Thailand.
[b] department of Chemistry and Biochemistry, University of South Carolina, Columbia, SC 29208, USA

Abstract

Copper(II) ion is one of the essential nutrients for the human body, but an excess of Cu^{2+} causes damage to the human cell and is implicated in many diseases. Cu^{2+} is also counted among heavy metal pollutants in the environment, especially in water. Thus a new approach towards quantifying Cu^{2+} ion is appealing. Here, we reported a new approach for Cu^{2+} detection with the combined concepts of ratiometric fluorescence and fluorescence resonance energy transfer (FRET). A new ratiometric mixed-QDs probe was employed for Cu^{2+} detection in an aqueous solution. This probe consists of highly photo stable blue-emitting Si QDs and yellow-emitting CdSe QDs. Si QDs act as a donor since the emission of Si QDs match with CdSe QDs absorbance. The energy transfer from Si QDs (donor) and CdSe QDs (acceptor) was confirmed by the time-resolved fluorescence. The changes in the ratiometric fluorescence response of the mixed-QDs probe upon exposure to Cu^{2+} were studied using fluorospectrometry, while the mechanism of the Cu^{2+} quenching to the probe was studied using an X-ray photoelectron spectrometer (XPS). This new Cu^{2+} detection approach provides a simple, fast, sensitive, accurate, low detection limit (3.89 nmol L^{-1}) with high selectivity to Cu^{2+} versus other biological relevant cations and cations of high environmental impacts. Furthermore, this new ratiometric mixed-QDs probe could be used as a naked-eye detection of Cu^{2+} for water samples and biological specimens with further development.

Introduction

Colloidal semiconductor nanocrystals (also called quantum dots,-QDs) have attracted much attention due to their unique optical and electronic properties. These properties include their tunable fluorescence and absorption spectra which can be attributed to quantum confinement. These properties have led to QDs being widely investigated in applications such as drug delivery[1-2], fluorescent markers for bioimaging[3-5], optical-electronic devices[6-7], immunoassays[8-10], and fluorescence-based sensing [4, 9, 11-28].

In recent years, QD-based fluorescence sensing has been targeted for the detection and measurement of biochemical conditions, pharmacological substances, and environmental pollutants with potential advantages in economy[27], sensitivity, and simplicity. The general schemes for fluorescent detection using QDs include 'turn-on' mechanisms, where the fluorescence intensity is enhanced by the addition of analytes, and 'Turn-off' mechanisms, in which quenching of fluorophores occurs in response to an analyte via direct quenching, photoinduced electron transfer (PET), and/or fluorescence resonance energy transfer (FRET) processes. Among QD compositions, there are many types that have been used for fluorescence sensing applications to date, notably including : CdSe[15, 21], CdSe/ZnS[22, 28], CdTe[17, 19, 25, 29], CdTe/ZnS[19], metal modified CdS[23], ZnSe/ZnS[26], $CuInS_2$[30], Si QDs[3-4, 9, 14, 24].

CdSe QDs are widely used as fluorescence probes due to their high photostability and tunability across the visible spectrum. CdSe QDs can be prepared mainly from two solvent systems: high boiling point organic solvents with coordinating surfactants, and aqueous-based systems. CdSe QDs that are prepared at high-temperature organic solvents

usually exhibit superior fluorescent properties, but often times a surface modification process is required to allow the QDs to be dispersible in water for further uses. In contrast, CdSe QDs prepared from water-based systems are readily water-dispersible when hydrophilic capping agents are used during the synthesis and can be natively attached to protect the QDs surface[31]. Some common stabilizing agents are 3-mercaptopropionic acid (MPA), L-glutathione (GSH), thioglycolic acid (TGA), and *N*-acetyl-L-cysteine (NAC). There have been many reports on the CdSe QDs that are prepared using water-based systems as it is relatively convenient in handling, but low photostability and sensitivity to variations in pH and ionic strength are of some concern.

In a similar vein, Si QDs have also been reported to be used in fluorescence sensing for the detection of various analyzes such as explosive molecules[32], organic compounds[33], alkaline phosphate[24], ethyl carbonate[9], glucose[34], and dyes[14] due to their high photostability, biocompatibility, low cytotoxicity, and surface paint-ability. Moreover, the preparation method of aqueous-based Si QDs is simple, low-cost, and non-toxic. To fabricate Si QDs-based fluorescence sensors, other molecules that are photoactive are usually required because Si QDs themselves have very high photostability and hardly respond to the analytes. There are a few reports using the organic molecules (in complementary to Si QDs) with aza crown[4] and azo group[14] to complete the electron transfer process, but to the best of our knowledge, there is no report on using Si QDs with other types of quantum dots. Furthermore, the emission energy of Si QDs is in the blue emission range which enables them to serve as a good energy donor for the other visible-emitting fluorophores in the photoinduced electron transfer (PET) and fluorescence resonance energy transfer (FRET) processes. In this work, we made use of the high photostability of blue-emitting Si QDs to design a new fluorescent probe.

Copper, while required as a nutrient, is identified as one of the toxic metals in water that can negatively affect animals, plants, and humans. An excess amount of copper in the human body can cause the risk of many diseases, such as Alzheimer's disease, prion disease, Wilson's disease and Parkinson's disease[27, 35-37]. The traditional methods for the detection of copper includes the use of inductively coupled plasma-mass spectroscopy (ICP-MS), inductively coupled plasma - optical emission spectrometry (ICP-OES), and atomic absorption spectroscopy (AAS). However, these techniques are expensive, time-consuming, and required skillful users. Therefore, the development of copper detection probes has received a big interest to be the simple, sensitive, fast, accurate, and low detection limit sensing probe. In recent years, the quantum dots-based fluorescence sensor has been widely studied for Cu^{2+} detection due to their high photostability[19, 21, 23, 25-28]. The detection of Cu^{2+} by fluorometric detection of QDs has been reported. Unfortunately, other metals ions such as Hg^{2+} and Ag^{+} also leads to the quenching of CdSe/ZnS QDs in the Cu^{2+} sensing system by the fluorometric detection of CdSe/ZnS.[28] This makes accurate determination of Cu^{2+} in any system more difficult. In addition, Mn^{2+} also "turn on" the fluorescence of Si QDs similar to Cu^{2+} thus, these Si QDs were used as a dual detection probe[27].

On the other hand, ratiometric fluorescence probes have been reported and showed significant improvement from the intensity-based systems for many reasons[38]. The ratiometric system, in which the ratio of fluorescence measured at two different emission and/or excitation wavelengths composes the signal, is self-correcting, so that interference from the probe concentration, media, and instrumental factors such as excitation power are eliminated. As a result, a separate internal standard is not required for the dual photoluminescence system, and complicated and high interference specimens such as biological samples can be readily analyzed. Also, naked-eye detection is promising for the ratiometric systems as the probes can give obvious changes of perceived emission color on exposure to the targeted condition or analyte. A ratiometric fluorescence probe for copper (II) ion detection has been reported by using CdTe QDs and metal-organic frameworks (MOFs)[17]. This ratiometric detection of CdSe/MOFs can overcome the effects of many interferences including Mn^{2+} and Ag^{+}, but the fluorescent signals can also be quenched by Hg^{2+} ions. Therefore, emitter combinations are required for ratiometric probes that have lower undesired quenching from interfering ions, and high photostability.

In this work, we report a new fluorescent probe consisting of mixed-QDs: Si QDs and CdSe QDs for sensitive and selective copper(II) ion detection in an aqueous solution. X-ray photoelectron spectroscopy (XPS) was measured to understand the quenching mechanism of the CdSe QDs which plays the dominant role in the mixed-QDs probe to detect Cu^{2+}. Blue-emitting Si QDs were selected as the FRET donor and yellow-emitting CdSe QDs as FRET acceptor. Naked eye detection of the analytes was done under a UV lamp by observing the change in emission colors. Our result opens door to the application of mixed Si QDs/CdSe QDs for naked eye Cu^{2+} detection in various analytes.

Experimental

1. Chemical

All chemicals were used without any furthur purification. Trisodium citrate dehydrate 99%, 3-(aminopropyl)trimethoxylsilane 97% (APTES) 3-mercatopropionic acid 98% (MPA), Hydrazine hydrate 99% ($N_2H_4 \cdot H_2O$), sodium hydroxide, (NaOH), N-[2- hydroxylethyl] piperazine-N'- [2-ethane-sulfonic acid] 99+ % (HEPES) were purchased from Sigma Aldrich. Cadmium chloride anhydrous, $CdCl_2$ > 99%, was from Fluka. Sodium selenite anhydrous 99% (Na_2SeO_3) was from Alfa Aesar. All the metal salts were analytical grade and purchased from Ajax Finechem, Thermo Fisher Scientific. Ultrapure water is used throughout (Milli-Q pure system, Millipore).

2. Instrumentation

Absorption spectra were recorded using a HP 8453 UV-VIS spectrophotometer. Fluorescence spectra measurements were done with a Cary Eclipse Fluorescence spectrophotometer at excitation = 350 nm. PerkinElmer, EnSight multimode microplate reader was used to analyze fluorescence intensity in selectivity study. Fluorescence lifetime of QDs were measured using Horiba DeltaFlex spectrophotometer Field emission transmission electron microscopic (FETEM) images of the quantum dots were captured using field emission transmission electron microscope: JEOL, JEM-3100F after depositing them on carbon-coated Cu grids. The elemental composition analysis was carried out by X-ray photoelectron spectrometer, XPS; AXIS ULTRADLD, Kratos analytical, Manchester UK. Fourier Transform Infrared, FTIR spectra were recorded by Thermo Scientific, Nicolet iS50 FTIR.

3. Syntheses

Si QDs synthesis

The synthesis of Si QDs was based on a reported method[3] with some modifications. Briefly, Si QDs were synthesized by the hydrothermal method. 1 g of tri-sodium citrate was dissolved in Milli Q water 21.5 mL and run through nitrogen gas for 15 min. Then 5.36 mL APTES was added into the solution. Finally, the mixture was transferred into a 100 mL Teflon-lined stainless-steel autoclave and heated at a constant temperature of 200 ºC for 4 h. Si QDs were purified by washing and centrifugation in ethanol several times. Si QDs were redispersed in Milli Q water and kept in the dark at 4 ºC for further use.

CdSe QDs synthesis

The synthesis of CdSe QDs was based on a reported method[15]. Typically, 0.80 mL of 0.20 M $CdCl_2$ solution was diluted in 50 mL of Milli Q water in the flask with a vigorous stir. Then, 34.6 µL of MPA was added into the solution followed by sufficient 1.0 M NaOH to adjust

the pH to 9.0. Then 0.80 mL of 0.02 M Na_2SeO_3 was injected into the flask. After the solution was refluxed at 100℃ for 5 min, 3.67 mL of $N_2H_4 \cdot H_2O$ was loaded into the solution. The yellow CdSe QDs solution was obtained after 12 h of refluxing at 100℃ under air. As-synthesized QDs were purified by washing with ethanol and centrifugation. Lastly, CdSe QDs were redispersed in Milli Q water and kept in the dark at 4 ºC for further use.

Mixed-QDs probe construction

300 µL of Si QDs (absorption value = 0.2, λ_{abs} = 350 nm) and 60 µL of CdSe QDs (absorption value = 0.15, λ_{abs} = 350 nm) were dissolved in 10 mM pH 7.0 HEPES buffer under the vigorous stirring. The final volume was adjusted to 3 mL to obtain the mixed-QDs probe solution for the further study.

4. Characterization of quantum dots

The optical properties of QDs were characterized by UV-VIS and fluorescence spectrometry. The sizes and planes of the dots were measured using the field emission transmission electron microscope (FETEM). The functional group of the dots was obtained by Fourier Transform Infrared (FTIR) technique.

5. Fluorescence titration

Quenching of Si and CdSe QDs by copper (II) ion was studied by fluorescent spectroscopy. 300 µL of Si QDs (in milli-Q water, absorption value = 0.2, λ_{abs} = 350 nm) and 60 µL of CdSe QDs (in milli-Q water, absorption value = 0.15, λ_{abs} = 350 nm) were transferred to the vial. Then the total volume was brought to 3 mL by the addition of 10 mM pH 7.0 HEPES buffer Then, a slight amount of Cu^{2+} ions from 10 mM $Cu(NO_3)_2$ was injected into the solution to give the final concentration of free copper ion as 0-16 µM.

The detection of Cu^{2+} by the mixed-QDs probe was studied by the fluorescence titration between mixed QDs-probe and Cu (II) ion solution at various concentrations from 0 nM – 200 nM.

6. Fluorescence lifetime analysis

PL lifetime analyses were conducted at room temperature using a Horiba DeltaFlex spectrophotometer with a 375nm pulsed laser diode excitation. Decay lifetimes were collected through a monochromator centered at either 485nm for Si QDs or 575nm for CdSe QDs with an emission bandwidth of 6nm and a time range of 100ns.

7. Selectivity study

In order to test the selectivity of the sensor for Cu^{2+}, the response to various metal ions including Co^{2+}, Fe^{3+}, Zn^{2+}, Al^{3+}, Mg^{2+}, Cr^{3+}, Ba^{2+}, Li^{+}, Ca^{2+}, Sr^{2+}, Ag^{+}, Na^{+}, Ni^{2+}, K^{+}, Cd^{2+}, Pb^{2+}, Mn^{2+}, and Hg^{2+}, was detected using the procedure below.

Selectivity of Si QDs, CdSe QDs, and mixed-QDs probe were studied. Separately Si QDs, CdSe QDs, and mixed-QDs probe with and without Cu^{2+} were added in 96 well plate. Then 6 µL 50 µM $Cu(NO_3)_2$ solution, or one of the other metals were added into each well, and the final volume of each well was adjusted to 300 µL by 10 mM HEPES buffer pH 7.0. The concentration of all metals was set at 1 µM. The plate was shaken automatically on the microplate reader for 15 min at 100 rpm before the fluorescence measurement.

Result and discussion

Characterization of as synthesized quantum dots

Si QDs was synthesized based on the previous report[3, 24] with modification in the heating system from using a microwave oven to a hydrothermal method under a Teflon-lined stainless-steel autoclave at 200 ℃. After 4 h, Si QDs were purified by ethanol. APTES was used as a silicon source for Si QDs with citrate as a stabilizing ligand. Blue-emitting Si QDs were obtained after the reaction and purification process. The UV-VIS absorption band and fluorescent spectra of Si QDs were illustrated in Figure 1. The characteristic first absorption peak of Si QDs at around 347 nm and the symmetric emission spectra at 430 nm corresponding to the blue emission color (Figure 4b) were obtained. In FTIR spectra, several distinct transmittance peaks appear in the range of 1000−3500 cm^{-1}. Typically, the broad absorption peaks at ~ 3120-3400 cm^{-1} is assigned to O-H stretching vibration. The absorption peak at ~ 1580-1650 cm^{-1} can be attributed to C=O stretching vibration indicated the production of –COOH and the absorbance at ~1390-1400 cm^{-1} is corresponding to C-O stretching vibration. Most importantly, the strong absorption peak at ~1100 cm^{-1} is ascribed to the Si-O bonding vibration stretching, which proved that Si QDs were successfully synthesized. Moreover, FETEM and SAED images in Figure 1c demonstrated the size, morphology, and crystal lattice of quantum dots. The average diameter of Si QDs is 2.50 **±** 0.30 nm with spherical particles and well dispersion. Additionally, the SAED image of Si QDs demonstrates the crystal lattice related to (111), (220), and (211) lattice planes with the d spacing equal to 3.14, 1.01, and 1.59 Å, respectively. The elemental analysis of these Si QDs by using energy-dispersive X-ray spectroscopy (EDS) proves that these Si QDs containing Si, C, O, and N. X-ray photoelectron spectroscopy (XPS) was used to study the surface composition of Si QDs. Full-scan XPS spectra of Si QDs, showed five distinct peaks at 1070 eV, 532 eV, 399 eV, 285 eV, and 102 eV which are related to Na 1s, O 1s, N 1s, C1s, and Si 2p, respectively, as shown in Figure 2a.

CdSe QDs were synthesized using hydrothermal method under the air atmosphere at 100 ℃ for 12 h in an aqueous solution without any shell coating based on the previous report[15]. Hydrazine was used as a reducing agent to reduce Se^{4+} to Se^{2-} without an oxygen-free atmosphere, and MPA was used as a stabilizing ligand to stabilize CdSe in an aqueous solution. A yellow-emitting CdSe QDs was obtained as shown in Figure 4. The obtained CdSe QDs were characterized by UV-VIS, fluorescence spectroscopy, FETEM, FTIR, and XPS measurement. Figure 1a shows the optical properties of CdSe QDs with the first absorption at around 549 nm and emission at 573 nm with a symmetric peak. The FETEM images of CdSe QDs showed well dispersion of spherical particles with an average diameter of 3.82 ± 0.77 nm. The SAED image illustrated the d-spacing of CdSe of 3.50, 2.14, 1.83 Å corresponding to (111), (220), and (311) lattice planes (Figure 1d.) The elemental analysis of these CdSe QDs using EDS represents the compositions of C, O, S, Se, and Cd. The FTIR spectra of CdSe QDs showed the transmittance peak at ~ 3120-3450, ~ 1586, ~ 1400 cm^{-1}, which were described to O-H stretching, C=O stretching vibration, and C-O stretching vibration, respectively. FTIR spectra demonstrated that CdSe QDs and Si QDs have many hydroxyl groups, Figure 1b. Full-scan XPS spectra of CdSe QDs (Figure 2b) showed six distinct peaks at 1072 eV, 532 eV, 405 eV, 295 eV, 168 eV and 54 eV which were corresponding to Na 1s, O 1s, Cd 3d, C 1s, S 2p and Se 3d, respectively. It is confirming the existence of Cd, Se, S in CdSe QDs.

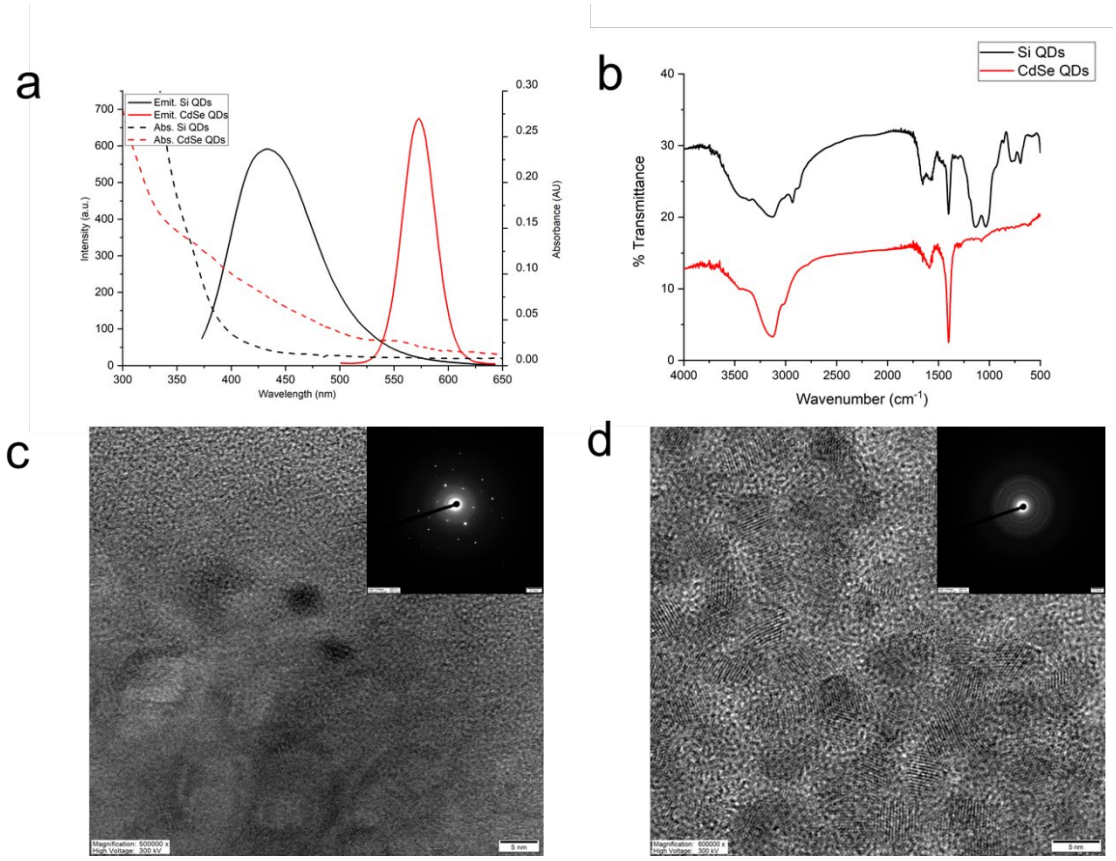

Figure 1. Absorbance and PL spectra (a), FTIR spectra (b), and FETEM images of Si QDs (c) and CdSe QDs (d).

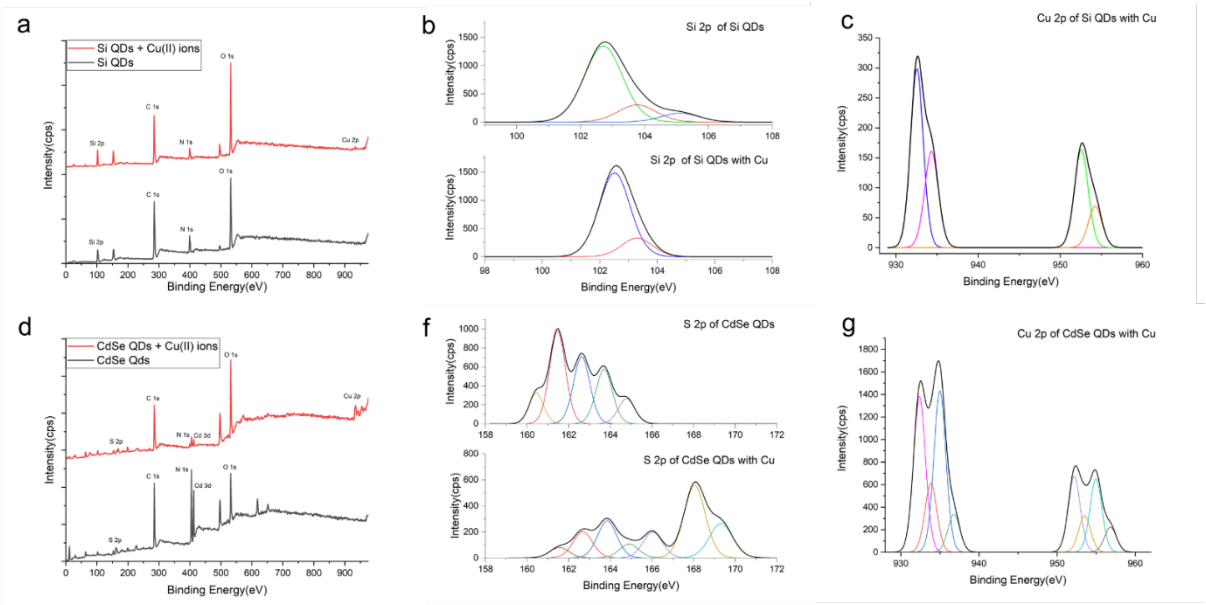

Figure 2. Full scan XPS spectra of Si QDs (a) and CdSe QD (d) and high-resolution XPS spectra of Si QDs at Si 2p (b), Cu 2p (c), of CdSe QDs at S 2p (f), and Cu 2p (g).

Quenching study: Detection of copper (II) ion

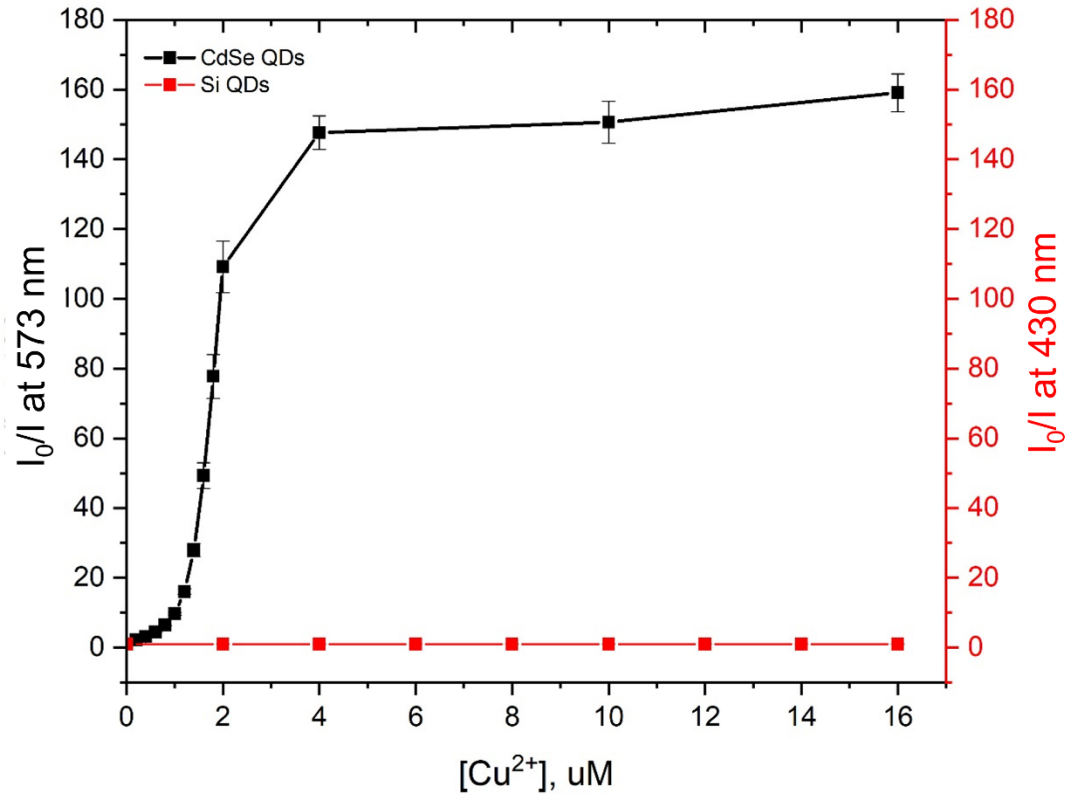

Figure 3. Stern-Volmer plot of CdSe QDs compared to Si QDs upon copper (II) quenching.

The quenching of Si QDs and CdSe QDs by Cu (II) ions were studied using fluorescence spectroscopy. Aliquots of CdSe QDs and Si QDs were dissolved in HEPES buffer 10 mM at pH = 7 and titrated with a small volume of copper (II) nitrate solution from 0.20 – 16.0 μM in the separate fluorescent cuvette. PL spectra of the titration provides information on the fluorescence intensity at the characteristic emission of CdSe QDs as shown in Figure S2. The fluorescent signals were gradually decreased upon the addition of copper (II) ion, while fluorescence intensity of Si QDs did not experience any significant change in the intensity at the same concentration of added Cu^{2+}.

The fluorescence quenching of CdSe QDs can be described by the Stern-Volmer equation as follow: $I_0/I = 1+K_{sv}[Q]$, where I_0 and I are the fluorescence intensity in the absence and presence of quencher, [Q] is quencher concentration and K_{SV} is a Stern-Volmer constant. The Stern-Volmer plot comparing the effect of Cu^{2+} ions to QDs in the concentration range from 0.2- 16 μM in Figure 3, indicating the clearly quenched of CdSe QDs in the presence of free copper (II) ions. Commonly, the quenching of fluorophore takes place through the static and/or dynamic interaction between fluorophore and quencher[26]. The deviations were observed at the higher concentration of Cu^{2+} which is probably related to the simultaneous existence of both statistic and dynamic quenching.[29]

The surface information of water dispersible CdSe QDs and Si QDs was investigated by X-ray photoelectron spectroscopy (XPS) analysis. XPS survey spectra of CdSe QDs and Si QDs were compared in the presence and absence of Cu^{2+} ions as shown in Figure 2a,d. The peak of Cu 2p was obviously observed at 932 eV for CdSe QDs, indicating the significant deposition of copper on the surface of CdSe QDs. On the other hand, XPS spectra of Si QDs exhibited only a tiny peak of Cu 2p. The observation of the different in copper composition on the surface can imply that copper (II) ions have higher tendency to deposit onto CdSe QDs

surface rather than Si QDs. This observation can be related to the possible mechanisms of the fluorescent quenching of CdSe QDs by Cu(II) ion as have been discussed previously as 1) the reduction of Cu (II) ion on the surface of CdSe QDs[25, 39-40], 2) Cation exchange on the surface of CdSe QDs[22], and 3) the K_{sp} of CuS, CuSe lower than CdSe[17, 25].

Detailed investigation on XPS analysis was done to better understand this phenomenon. The XPS spectra of CdSe in the presence of Cu^{2+} ions demonstrated that Cd (II) ions remained on the surface, but they were disturbed by Cu (II) ion as the intensity of the main Cd peak decreased with slight redshift on the binding energy (Figure S3), while in Si QDs, only small tail loss (Figure 2b.) It can be implied that Cu (II) ions bound more effectively on the surface of CdSe QDs than Si QDs. Furthermore, at Cu 2p of high-resolution XPS spectra of CdSe (Figure 2g), various species of Cu including Cu^0, Cu^+, and Cu^{2+} were detected, but they were not observed in Si QDs. This observation can be related to the partial reduction of Cu^{2+} on the surface of CdSe QDs into Cu^+ and Cu^0, and Cd^{2+} on the surface can then be replaced by Cu ions that were reduced. Moreover, that high-resolution XPS at S 2p (Figure 2f) demonstrated the oxidation of $S^{2-}$and -SH on the surface of QDs to sulfate and thiosulphate at 168.0 and 169.3 eV. Another reason for the high ability of Cu^{2+} in quenching of CdSe QDs could be the formation of CuS on the surface of CdSe QDs leading to non-radiative process for the exciton as the K_{sp} of CuS (6.0×10^{-37})[17] is lower than K_{sp} of CdSe (6.3×10^{-36})[22]. In comparison to the XPS analysis of Si QDs, the high-resolution XPS of Si QDs at Cu 2p illustrated the existence of Cu on the surface of QDs, but with lower intensity than on CdSe QDs. The reason for small Cu deposition could be that the functional group on Si QDs was mainly carbonyl group from sodium citrate capping agent, which has lower binding affinity with Cu^{2+}. Upon the detailed investigation in combination with the fluorescence titration and Stern-Volmer's plot, it can be inferred that Cu^{2+} mainly quench CdSe QDs but not Si QDs. The different effects of Cu (II) ions on Si QDs and CdSe QDs leads us to the idea of naked eyes Cu^{2+} sensing probe called a mixed QDs probe.

Copper detection method by mixed QDs probe

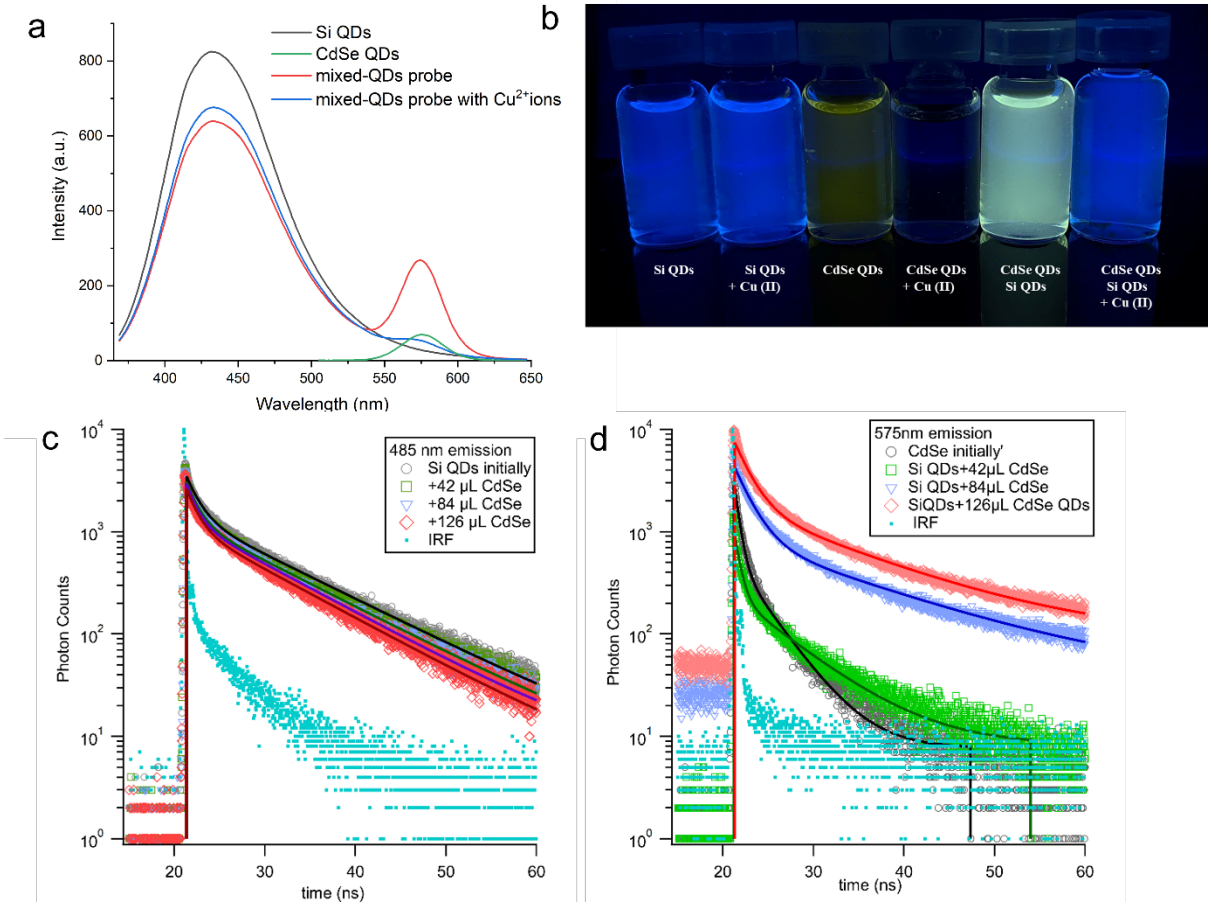

Figure 4. PL spectra of mixed QDs probe titrate with Cu^{2+} (a), and Si QDs, CdSe QDs, mixed QDs probe in presence and absence of Cu^{2+} under UV lamp (b). Lifetime of Si QDs initially and after addition of CdSe QDs (probe at 485nm) (c). and lifetime of CdSe QDs initially and after addition of CdSe QDs to Si QDs (probe at 575nm). Solid lines represent the fit.

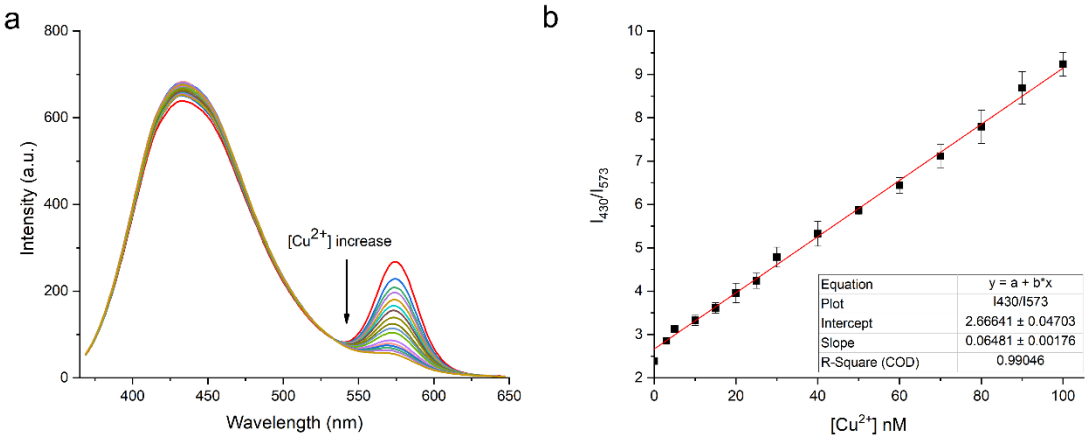

Figure 5. fluorescence titration spectra of the mixed-QDs probe with Cu^{2+} ion (a), and ratio plot of mixed-probe versus [Cu^{2+}] (b).

Since CdSe QDs were dramatically quenched and Si QDs were rarely affected by Cu^{2+} ions, ratiometric fluorescence sensor combining Si QDs and CdSe were created. Mixed-QD probe was fabricated in 10 mM HEPES buffer (pH = 7.0) by mixing the two QDs in the buffer. The mixed-QDs probe exhibited compatibility between the two aqueous QDs without the induction of precipitation. FETEM image of the mixed-QDs probe provided information on the particle size and morphology of the probe as homogeneous mixing of the two dots and without any coating or aggregation of mixed dots observed (Figure S6.) The EDS analysis showing that this mixed probe contains Cd, Se, Si, S, C, N, and O as shown in Table S5 . The emission color of the mixed-QDs probe was yellow-green and was significantly brighter than CdSe QDs, Figure 4b.

The mixed-QDs probe showed 2 emission spectra at 430 and 573 nm belonging to Si QDs and CdSe QDs, respectively. However, we observed an enhancement of fluorescence spectra of CdSe QDs at 573 nm when Si QDs are added as shown in Figure 4.

Fluorescence resonance energy transfer, FRET, a non-radiative process between two fluorescence molecules was expected to be the reason for enhancement in CdSe fluorescence. FRET relies that the distance between the donor molecule (D) and the acceptor molecule (A) is typically of the order 1-10 nm[10, 41]. For FRET to occur, there are few criteria needed. First, the spectra emission of D must overlap with the absorption of A. Also, the proximity between D and A should be about 10 Å to 100 Å [42-43]. The size of our QDs and the overlap between the emission spectra of Si QDs and absorption spectra of CdSe QDs clearly satisfied the FRET criteria. To confirm the energy transfer between Si QDs and CdSe QDs, fluorescence titration between Si QDs and CdSe QDs was studied in detail as shown in Figure S4. We carried out two titration experiments to confirm the energy transfer between Si QDs and CdSe QDs, 1) CdSe QDs were titrated with Si QDs and 2) Si QDs were titrated with CdSe QDs. The results showed that PL intensity of CdSe QDs were enhanced with the increasing amount of Si QDs, and the PL intensity of Si QDs were diminished with the increasing amount of CdSe QDs, confirming the energy transfer from Si QDs (donor) to CdSe QDs (acceptor) at the excitation of Si QDs (350 nm).

To further confirm the presence of energy transfer, time-resolved (TR) PL measurements were done using 375 nm pulsed laser diode excitation. To separately resolve emission from the Si QDs and CdSe QDs, we probed two different emission channels selected by a monochromator. Figure 4c shows the TR-PL signal at 485nm where the emission is dominated by Si QDs, while Figure 4d shows the signal at 575nm where the emission is dominated by the CdSe QDs once they are introduced. Both sets of decays were fit with biexponential functions, from which the decay lifetime τ_D is expressed as the amplitude average lifetime. The initial samples of Si QDs (donor) have an amplitude average lifetime of 4.8±0.11ns, while that of the CdSe (acceptor) was determined to be 1.0±0.12ns. In the presence of energy transfer from the Si QDs (donor) to the CdSe QDs (acceptor), we will expect the average lifetime of the donor to decrease[44]. Specifically, because the Si QD lifetime is significantly longer than the CdSe QDs lifetime, we expect the lifetime measured at the CdSe QD emission channel to increase when the QDs are additionally excited via energy transfer from the Si QDs, approaching the lifetime recorded at the Si emission channel. Upon addition of CdSe QDs to the Si QDs, the amplitude average lifetime of the Si QDs (donor) continues to decrease with each aliquots addition of CdSe with a corresponding increase in the average lifetime of that of the CdSe QDs (acceptor) as shown Table S1. After the final addition of the CdSe QDs (reaching 0.25μM CdSe QDs), the amplitude average lifetime of the donor (Si QDs) has decreased to 4.3±0.17ns while that of the acceptor (CdSe QDs) has increased to 4.1±0.32ns as shown in the Figure 4c and Table S2. Given the low optical density of the sample, this is clear evidence of non-radiative energy transfer from the Si QDs to the CdSe QDs.[45-46] In addition to this and to corroborate the quenching of the CdSe in the presence of Cu^2 we added successive aliquots of Cu^{2+} to the mixed QD sensor solution. As shown Figure S5, the lifetime of the CdSe QDs continued to diminish with each addition of Cu^{2+} ions to the mixture. This further confirms that the CdSe QDs is strongly quenched in the presence of Cu^{2+} ions.

Fluorescence technique was used to indicate the detection of Cu^{2+} ions by the mixed QDs probe. The diminish of fluorescence intensity at 573 nm was observed upon the addition of Cu^{2+} ions. This can be attributed to the effect of Cu^{2+} ions on the CdSe QDs surface (Figure 5a.) The ratiometric plot: I_{430}/I_{573} versus concentration of quencher, Cu^{2+} (Figure 5b) showed that there was a linear relationship between the concentration of Cu^{2+} ion and: I_{430}/I_{573} value in the range of 0-100 nM (R^2 = 0.99046). The mixed-QDs probe has a detection limit of 3.89 nM, which was almost 10 times lower than the CdSe (MPA) QDs based sensor published previuosly[21]. The reasons for the high sensitivity of this probe were likely the combination from the sensitivity from using intensity ratio and the increase of CdSe QDs fluorescent signals due to FRET.

Another purpose of implementation of the mixed-QDs probe for sensing Cu^{2+} is the ability for naked eye detection. In the presence of 10 μM of Cu^{2+}, under a UV lamp, the mixed-QDs sensor changes the emission color from yellow-green to blue as shown Figure 4b.

Selectivity study: interference test

In addition to Cu^{2+} ions, the fluorescence quenching of mixed QDs-probe was also evaluated in the presence of some relevant biological cations and cations of environmental problem concerns: Ag^{+},Fe^{3+}, Ni^{2+}, Cr^{3+},Co^{2+}, Ca^{2+}, Li^{+}, Mg^{2+}, Sr^{2+}, Al^{3+}, Ba^{2+}, Zn^{2+}, Na^{+}, K^{+}, Pb^{2+}, Mn^{2+}, Cd^{2+}, and Hg^{2+}, as shown in Figure 6. The fluorescent ratio (I_{430}/I_{573}) of the mixed-QDs probe increased significantly when exposed to 1 μM Cu^{2+} ions, whereas the exposure to the same concentration of other cations caused slightly changes (~20 times lower), shown in Figure 6a. In the presence of 1 μM Cu^{2+} ions, other cations did not change the intensity ratio as well. These observations indicated the good selectivity of Cu^{2+} ions compared with the other competitive cations.

The selectivity of the mixed-QDs probe to Cu^{2+} ions are due to the reasons mentioned earlier including the deposition of CuS and/or substitution of Cd^{2+} ion by Cu^{2+} ion leading to the non-radiative recombination of exciton. From the hard-soft acid-base theory, Cu^{2+} ion has Pearson border acid character which has a strong interaction with thiol groups[47]. Other metals with hard and borderline acid characters could bind to both carboxylate group of MPA on CdSe QDs and citrate group on Si QDs, and did not lead to the deposition of metal salts on QDs surface. Only in the presence of Cu^{2+} ions, the thiol group of MPA will react with Cu^{2+} ions to form CuS[17] leading to the quenching of luminescence[26].

To demonstrate that the mixed-QDs probe can be used as the naked eye detection with selectivity to Cu^{2+}, Figure 6b illustrates the changes in emission color comparing of Si QDs, CdSe, QDs, mixed-QDs probe (with and without Cu). The yellow-green emission of probe completely turn to blue emission upon the addition of Cu^{2+} while it is remaining yellow-green by the addition of the other cations.

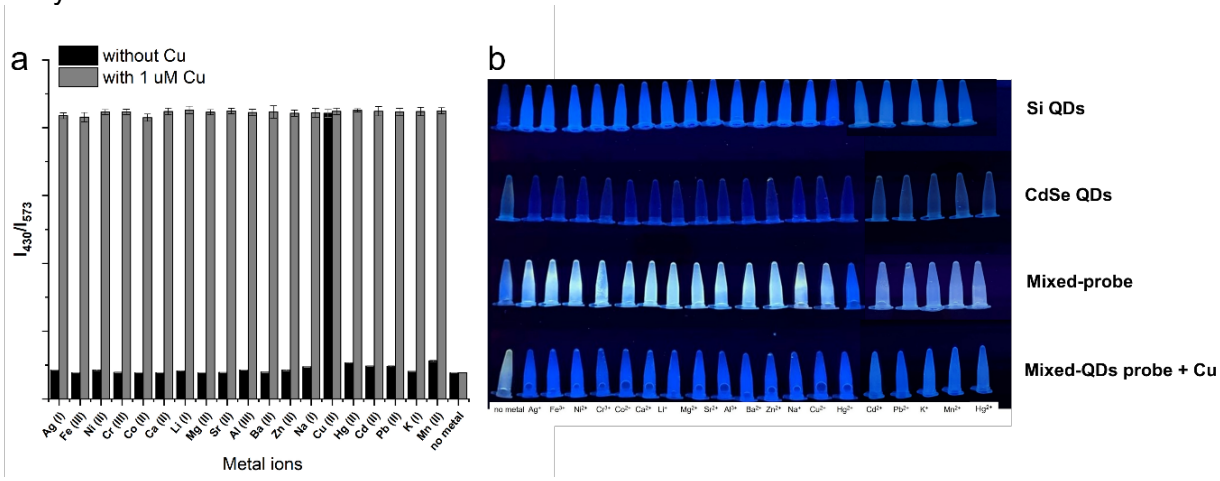

Figure 6. selectivity study of mixed-QDs probe comparing the absence and internal Cu^{2+} adding (a), and interferences study under UV-lamp (ex 365 nm) (b).

Table 1. shows the comparison of Cu sensing based on quantum dots

Entry	Sensor	Analyze	LOD (nM)	Reported tolerated metal ions	Linear range	REF
1	CdSe/ZnS (BSA)	Cu^{2+} Fe^{3+}	10	Ca^{2+}, K^{+}, Na^{+}, Mg^{2+}, Mn^{2+}, Zn^{2+}, Fe^{3+}	0.01-2μM	22
2	CdSe/ZnS (CTAB)	Cu^{2+}	0.15	Zn^{2+}, Pb^{2+}, In^{3+}, Fe^{3+}, Co^{2+}, Cd^{2+}, Ca^{2+}; Hg^{2+}, Ag^{+}	N/A	28
3	CdTe(TGA)	Cu^{2+}	0.04	Pb^{2+}, Hg^{2+}, Ca^{2+}, Zn^{2+}, Cd^{2+}, Mg^{2+}, K^{+}, Na^{+}, Ag^{+}, Fe^{3+}	0.25-617.53 nM	25
4	CdTe(TGA) + MOF	Cu^{2+}	4.09	Mg^{2+}, Pb^{2+}, Co^{2+}, Ba^{2+}, $Mn^{2=}$, Fe^{3+}, Cr^{6+}, Zr^{4+}, Ca^{2+}, Ag^{+}, Hg^{2+}	4.0-40.0 ng/ml	17
5	CdSeTe QD (cys)	Cu^{2+}	7.1	$Pb^{2+,}$Fe2+ K^{+}, Na^{+}, Mg^{2+}, Al^{3+}, Ca^{2+}, Zn^{2+}.	20nM-2uM	48
6	CdTe/ZnS	Cu^{2+}	1.50	Ag^{+}, Hg^{2+}, Co^{2+}, Ba^{2+}, Zn^{2+}, Al^{3+}, Cd^{2+}, Ni^{2+}, Ca^{2+}, Mg^{2+}, Mn^{2+}, Pb^{2+}, Na^{+}, K^{+}, Cr^{3+}, Fe^{2+}, Fe^{3+}	2.5 nM-1.75 μM	19
7	CdSe (MPA)	Cu^{2+}	30	Fe^{3+}, Zn^{2+}, Ag^{+}, Mn^{2+}, Co^{2+}, Hg^{2+}, Pb^{2+}	30 nM-3 μM	21
8	ZnSe (MPA)	Cu^{2+}	170	Al^{3+}, Ba^{2+}, Ca^{2+}, Fe^{3+}, K^{+}, Mg^{2+}, Mn^{2+}, Na^{+}, NH_4^{+}, Zn^{2+}	0.059 – 9.84 μM	26
9	CdS QDs	Cu^{2+}	10	K^{+}, Na^{+}¸Ca^{2+}, Mg^{2+}, Zn^{2+}, Mn^{2+}, Fe^{3+}, Co^{2+}	0.02 – 2.0 μM	23
10	Mixed-QDs probe (CdSe-Si QDs)	Cu^{2+}	3.89	Ag^{+},Fe^{3+}, Ni^{2+}, Cr^{3+},Co^{2+}, Ca^{2+}, Li^{+}, Mg^{2+}, Sr^{2+}, Al^{3+}, Ba^{2+}, Zn^{2+}, Na^{+}, K^{+}, Pb^{2+}, Mn^{2+}, Cd^{2+}, Hg^{2+}	0-100 nM	This work

Conclusion

This work has demonstrated the ratiometric fluorescence sensor for rapid, sensitive, and selective to Cu^{2+} ions using the mixed-QDs probe in an aqueous solution. The mixed-QDs probe consists of two types of QDs are CdSe QDs and Si QDs without any modification on the surface. Mixed QDs probe has good solubility in aqueous without any accumulation. The yellow-green emission of mixed-QDs probe originated from the yellow-emitting CdSe QDs and blue emitting Si QDs. In the presence of Cu^{2+} ions, the emission color would turn to blue. The detection limit was 3.89 nmol L^{-1} for Cu^{2+} ions with the linear range from 0-100 nmol L^{-1} (R^2 = 0.99046). The mixed-QDs probe has a good sensitivity and selectivity toward to the biological relevant cations and cations of environmental concern: Ag^{+}, Fe^{3+}, Ni^{2+}, Cr^{3+},Co^{2+}, Ca^{2+}, Li^{+}, Mg^{2+}, Sr^{2+}, Al^{3+}, Ba^{2+}, Zn^{2+}, Na^{+}, K^{+}, Pb^{2+}, Mn^{2+}, Cd^{2+}, and Hg^{2+}. The detection limit and linear range of this mixed-QDs probe are comparable with other QDs probes reported previously, with the advantage of the large range of other metal cations that this probe can tolerate as shown in Table 1.

The mixed-QDs probe demonstrates the ratiometric fluorescent probe with only QDs-based fluorophores. Photostability, sensitivity, selectivity and ability for naked eye detection of Cu^{2+} could allow this probe system to be further developed for use in analysis of water samples and biological specimens.

Acknowedgements (Greytak group): ABG and SA acknowledge additional support from US NSF (CHE-2109064).

References

1. Chen, X.; Tang, Y.; Cai, B.; Fan, H., 'One-pot' synthesis of multifunctional GSH–CdTe quantum dots for targeted drug delivery. *Nanotechnology* **2014,** *25* (23), 235101.
2. Ki, D.; Sohn, H., Water Soluble Silicon Quantum Dots Grafted with Amoxicillin as a Drug Delivery System. *J Nanosci Nanotechnol* **2020,** *20* (8), 4624-4628.
3. Zhong, Y.; Peng, F.; Bao, F.; Wang, S.; Ji, X.; Yang, L.; Su, Y.; Lee, S. T.; He, Y., Large-scale aqueous synthesis of fluorescent and biocompatible silicon nanoparticles and their use as highly photostable biological probes. *J Am Chem Soc* **2013,** *135* (22), 8350-6.
4. Dhenadhayalan, N.; Lee, H. L.; Yadav, K.; Lin, K. C.; Lin, Y. T.; Chang, A. H., Silicon Quantum Dot-Based Fluorescence Turn-On Metal Ion Sensors in Live Cells. *ACS Appl Mater Interfaces* **2016,** *8* (36), 23953-62.
5. Shu, C.; Huang, B.; Chen, X.; Wang, Y.; Li, X.; Ding, L.; Zhong, W., Facile synthesis and characterization of water soluble ZnSe/ZnS quantum dots for cellar imaging. *Spectrochim Acta A Mol Biomol Spectrosc* **2013,** *104*, 143-9.
6. Zhang, Q.; Zhang, Y.; Huang, S.; Huang, X.; Luo, Y.; Meng, Q.; Li, D., Application of carbon counterelectrode on CdS quantum dot-sensitized solar cells (QDSSCs). *Electrochemistry Communications* **2010,** *12* (2), 327-330.
7. Poly, L. P.; Mace, B.; Kottokkaran, R.; Bagheri, B.; Noack, M.; Dalal, V. In *Novel CdSe Solar Cell*, 2021 IEEE 48th Photovoltaic Specialists Conference (PVSC), 20-25 June 2021; 2021; pp 0443-0446.
8. Speranskaya, E. S.; Beloglazova, N. V.; Lenain, P.; De Saeger, S.; Wang, Z.; Zhang, S.; Hens, Z.; Knopp, D.; Niessner, R.; Potapkin, D. V.; Goryacheva, I. Y., Polymer-coated fluorescent CdSe-based quantum dots for application in immunoassay. *Biosens Bioelectron* **2014,** *53*, 225-31.
9. Luo, L.; Song, Y.; Zhu, C.; Fu, S.; Shi, Q.; Sun, Y.-M.; Jia, B.; Du, D.; Xu, Z.-L.; Lin, Y., Fluorescent silicon nanoparticles-based ratiometric fluorescence immunoassay for sensitive detection of ethyl carbamate in red wine. *Sensors and Actuators B: Chemical* **2018,** *255*, 2742-2749.
10. Medintz, I. L.; Mattoussi, H., Quantum dot-based resonance energy transfer and its growing application in biology. *Phys Chem Chem Phys* **2009,** *11* (1), 17-45.
11. Tomokazu, K.; Nayuta, F.; Takeshi, F.; Miho, S., CdSe/ZnS Quantum Dots Conjugated with a Fluorescein Derivative: a FRET-based pH Sensor for Physiological Alkaline Conditions. *ANALYTICAL SCIENCES* **2014,** *30*.
12. Jin, T.; Sasaki, A.; Kinjo, M.; Miyazaki, J., A quantum dot-based ratiometric pH sensor. *Chem Commun (Camb)* **2010,** *46* (14), 2408-10.
13. Chu, B.; Wang, H.; Song, B.; Peng, F.; Su, Y.; He, Y., Fluorescent and Photostable Silicon Nanoparticles Sensors for Real-Time and Long-Term Intracellular pH Measurement in Live Cells. *Anal Chem* **2016,** *88* (18), 9235-42.
14. Jose, A. R.; Sivasankaran, U.; Menon, S.; Kumar, K. G., A silicon nanoparticle based turn off fluorescent sensor for sudan I. *Analytical Methods* **2016,** *8* (28), 5701-5706.
15. Chen, A.; Peng, X.; Pan, Z.; Shao, K.; Wang, J.; Fan, M., Visual Assay of Glutathione in Vegetables and Fruits Using Quantum Dot Ratiometric Hybrid Probes. *J Agric Food Chem* **2018,** *66* (25), 6431-6438.
16. Soheyli, E.; Sahraei, R.; Nabiyouni, G.; Nazari, F.; Tabaraki, R.; Ghaemi, B., Luminescent, low-toxic and stable gradient-alloyed Fe:ZnSe(S)@ZnSe(S) core:shell quantum dots as a sensitive fluorescent sensor for lead ions. *Nanotechnology* **2018,** *29* (44), 445602.
17. Yang, Y.; Liu, W.; Cao, J.; Wu, Y., On-site, rapid and visual determination of Hg(2+) and Cu(2+) in red wine by ratiometric fluorescence sensor of metal-organic frameworks and CdTe QDs. *Food Chem* **2020,** *328*, 127119.
18. Zhang, J.; Yu, S. H., Highly photoluminescent silicon nanocrystals for rapid, label-free and recyclable detection of mercuric ions. *Nanoscale* **2014,** *6* (8), 4096-101.
19. Bian, W.; Wang, F.; Zhang, H.; Zhang, L.; Wang, L.; Shuang, S., Fluorescent probe for detection of Cu^{2+} using core-shell CdTe/ZnS quantum dots. *Luminescence* **2015,** *30* (7), 1064-70.
20. Wang, G.; Yau, S.; Mantey, K.; Nayfeh, M. H., Fluorescent Si nanoparticle-based electrode for sensing biomedical substances. *Optics Communications* **2008,** *281* (7), 1765-1770.

21. Shiqi, J.; Zifan, L.; Tiantian, S.; Yanting, F.; Chunxia, Z.; Pengzhi, H.; Shengli, S.; Chengyong, L., High Sensitivity Detection of Copper Ions in Oysters Based on the Fluorescence Property of Cadmium Selenide Quantum Dots. *Chemosensors* **2019,** *7* (4), 47.
22. Xie, H.; Liang, J.; Zhan, Z.; Liu, Y.; He, Z.; Pang, D., Luminescent CdSe-ZnS quantum dots as selective Cu^{2+} probe. *Spectrochimica Acta Part A: Molecular and Biomolecular Spectroscopy* **2004,** *60* (11), 2527-2530.
23. Wang, G. L.; Dong, Y. M.; Li, Z. J., Metal ion (silver, cadmium and zinc ions) modified CdS quantum dots for ultrasensitive copper ion sensing. *Nanotechnology* **2011,** *22* (8), 085503.
24. Li, Z.; Ren, X.; Hao, C.; Meng, X.; Li, Z., Silicon quantum dots with tunable emission synthesized via one-step hydrothermal method and their application in alkaline phosphatase detection. *Sensors and Actuators B: Chemical* **2018,** *260*, 426-431.
25. Wang, A.; Fu, L.; Rao, T.; Cai, W.; Yuen, M.; Zhong, J., Effect of metal ions on the quenching of photoluminescent CdTe QDs and their recovery. *Optical Materials* **2015,** *42*, 548-552.
26. Passos, S. G. B.; Kunst, T. H.; Freitas, D. V.; Navarro, M., Paired electrosynthesis of ZnSe/ZnS quantum dots and Cu2+ detection by fluorescence quenching. *Journal of Luminescence* **2020,** *228*, 117611.
27. Zhu, B.; Tang, M.; Yu, L.; Qu, Y.; Chai, F.; Chen, L.; Wu, H., Silicon nanoparticles: fluorescent, colorimetric and gel membrane multiple detection of Cu^{2+} and Mn^{2+} as well as rapid visualization of latent fingerprints. *Analytical Methods* **2019,** *11* (28), 3570-3577.
28. Jin, L. H.; Han, C. S., Ultrasensitive and selective fluorimetric detection of copper ions using thiosulfate-involved quantum dots. *Anal Chem* **2014,** *86* (15), 7209-13.
29. Peng, C.; Zhang, Y.; Qian, Z.; Xie, Z., Fluorescence sensor based on glutathione capped CdTe QDs for detection of Cr^{3+} ions in vitamins. *Food Science and Human Wellness* **2018,** *7* (1), 71-76.
30. Lin, Z.; Ma, Q.; Fei, X.; Zhang, H.; Su, X., A novel aptamer functionalized CuInS2 quantum dots probe for daunorubicin sensing and near infrared imaging of prostate cancer cells. *Anal Chim Acta* **2014,** *818*, 54-60.
31. Zhu, H.; Hu, M. Z.; Shao, L.; Yu, K.; Dabestani, R.; Zaman, B.; Liao, S., Synthesis and Optical Properties of Thiol Functionalized CdSe/ZnS (Core/Shell) Quantum Dots by Ligand Exchange. *Journal of Nanomaterials* **2014,** *2014*, 1-14.
32. Kim, J. S.; Cho, B.; Cho, S. G.; Sohn, H., Silicon quantum dot sensors for an explosive taggant, 2,3-dimethyl-2,3-dinitrobutane (DMNB). *Chem Commun (Camb)* **2016,** *52* (53), 8207-10.
33. Nguyen, A.; Gonzalez, C. M.; Sinelnikov, R.; Newman, W.; Sun, S.; Lockwood, R.; Veinot, J. G.; Meldrum, A., Detection of nitroaromatics in the solid, solution, and vapor phases using silicon quantum dot sensors. *Nanotechnology* **2016,** *27* (10), 105501.
34. Yi, Y.; Deng, J.; Zhang, Y.; Li, H.; Yao, S., Label-free Si quantum dots as photoluminescence probes for glucose detection. *Chem Commun (Camb)* **2013,** *49* (6), 612-4.
35. Bisaglia, M.; Bubacco, L., Copper Ions and Parkinson's Disease: Why Is Homeostasis So Relevant? *Biomolecules* **2020,** *10* (2), 195.
36. Purchase, R., The Link between Copper and Wilson's Disease. *Science Progress* **2013,** *96* (3), 213-223.
37. Varela-Nallar, L.; González, A.; Inestrosa, N. C., Role of Copper in Prion Diseases: Deleterious or Beneficial? *Current Pharmaceutical Design* **2006,** *12*, 2587-2595.
38. Somers, R. C.; Bawendi, M. G.; Nocera, D. G., CdSe nanocrystal based chem-/bio- sensors. *Chem Soc Rev* **2007,** *36* (4), 579-91.
39. Alex, V.; Isarov; John, C., Optical and Photochemical Properties of
Nonstoichiometric Cadmium Sulfide Nanoparticles: Surface Modification with Copper(II) Ions. *Langmuir* **1997,** *13*.
40. Knowles, K. E.; Hartstein, K. H.; Kilburn, T. B.; Marchioro, A.; Nelson, H. D.; Whitham, P. J.; Gamelin, D. R., Luminescent Colloidal Semiconductor Nanocrystals Containing Copper: Synthesis, Photophysics, and Applications. *Chem. Rev.* **2016**.
41. Hoffman, R. M., Cell Markers: Green Fluorescent Protein. **2013**, 483-487.

42. Randee, J. M. B., FRET Study of Ligand Binding and Exchange Kinetics on the Surface of CdSe/ZnS Quantum Dots. *Theses and Dissertations* **2015,** *7*, 1267.
43. Maria, C.; Chirio, L.; Michel, P., Fluorescence resonance energy transfer (FRET): theory and experiments. *Biochcfnical Education* **1998,** *26*, 320-323.
44. Hildebrandt, N.; Spillmann, C. M.; Algar, W. R.; Pons, T.; Stewart, M. H.; Oh, E.; Susumu, K.; Díaz, S. A.; Delehanty, J. B.; Medintz, I. L., Energy Transfer with Semiconductor Quantum Dot Bioconjugates: A Versatile Platform for Biosensing, Energy Harvesting, and Other Developing Applications. *Chemical Reviews* **2017,** *117* (2), 536-711.
45. Kagan, C. R.; Murray, C. B.; Nirmal, M.; Bawendi, M. G., Electronic Energy Transfer in CdSe Quantum Dot Solids. *Physical Review Letters* **1996,** *76* (9), 1517-1520.
46. Kagan, C. R.; Murray, C. B.; Bawendi, M. G., Long-range resonance transfer of electronic excitations in close-packed CdSe quantum-dot solids. *Physical Review B* **1996,** *54* (12), 8633-8643.
47. Pearson, R. G., Hard and Soft Acids and Bases, HSAB, Part I. *Journal of Chemical Education* **1968,** *45* (9).
48. Liang, G. X.; Liu, H. Y.; Zhang, J. R.; Zhu, J. J., Ultrasensitive Cu^{2+} sensing by near-infrared-emitting CdSeTe alloyed quantum dots. *Talanta* **2010,** *80* (5), 2172-6.

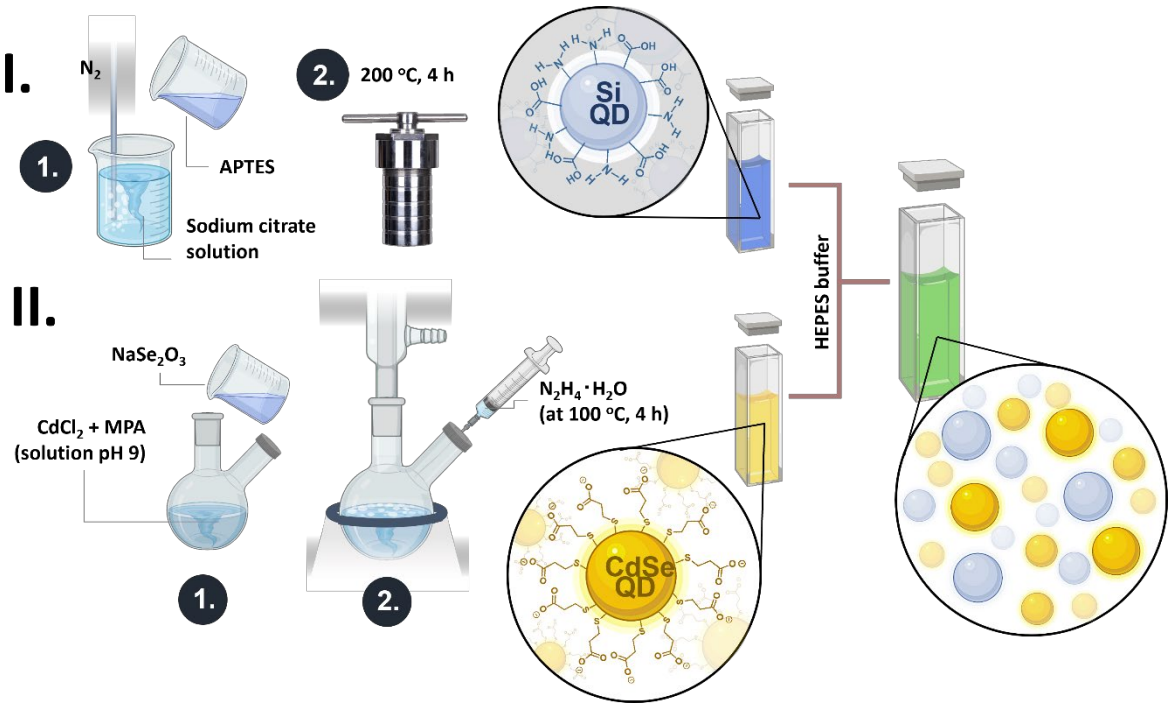

Figure S1. Schematic illustration of the fabrication of mixed-QDs probe

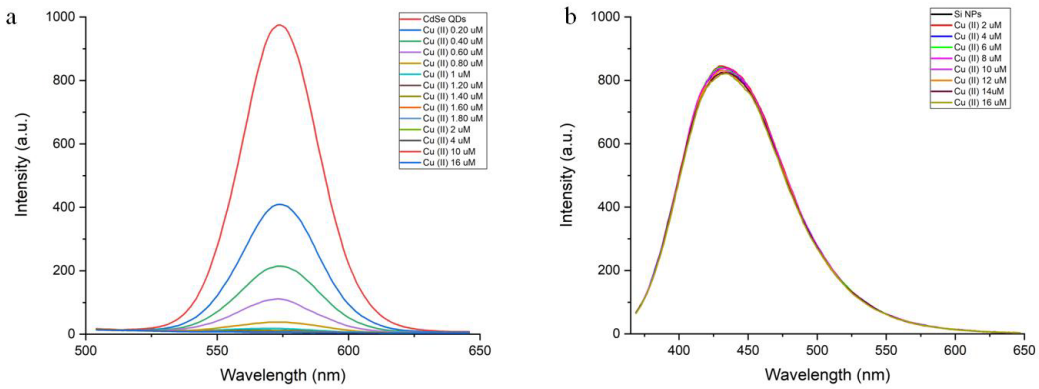

Figure S2. fluorescence spectra of CdSe QDs (a) and Si QDs (b) while adding Cu^{2+} ion.

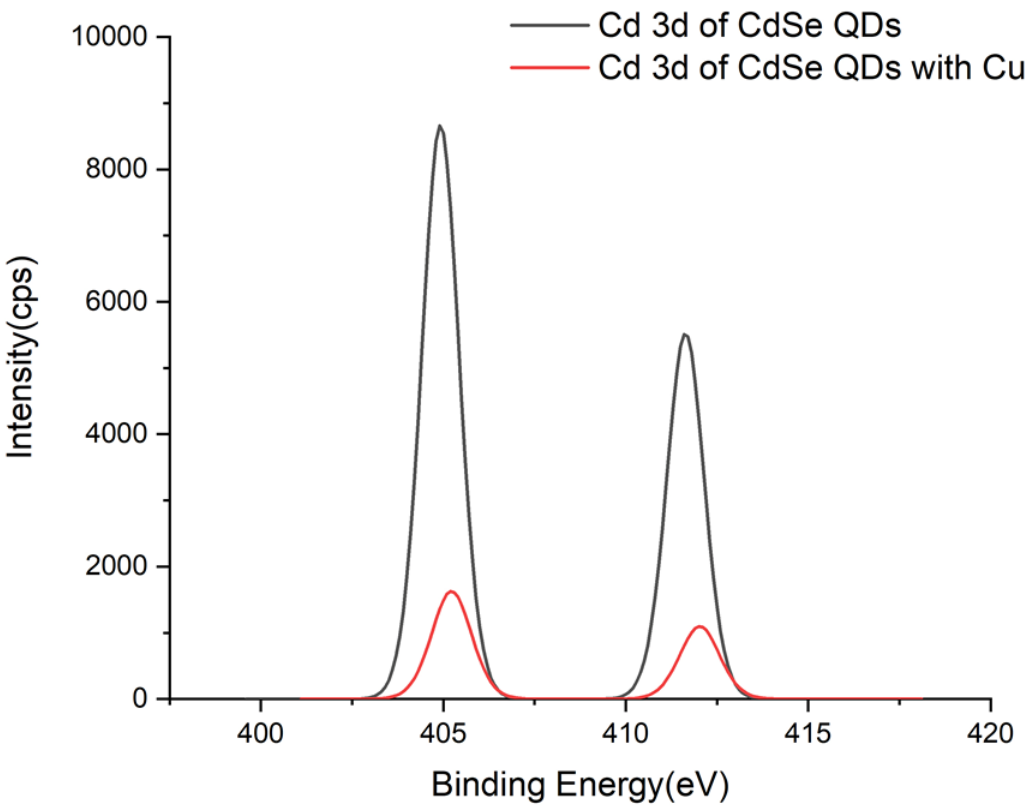

Figure S3. High-resolution XPS spectra of CdSe QDs at Cd 3d.

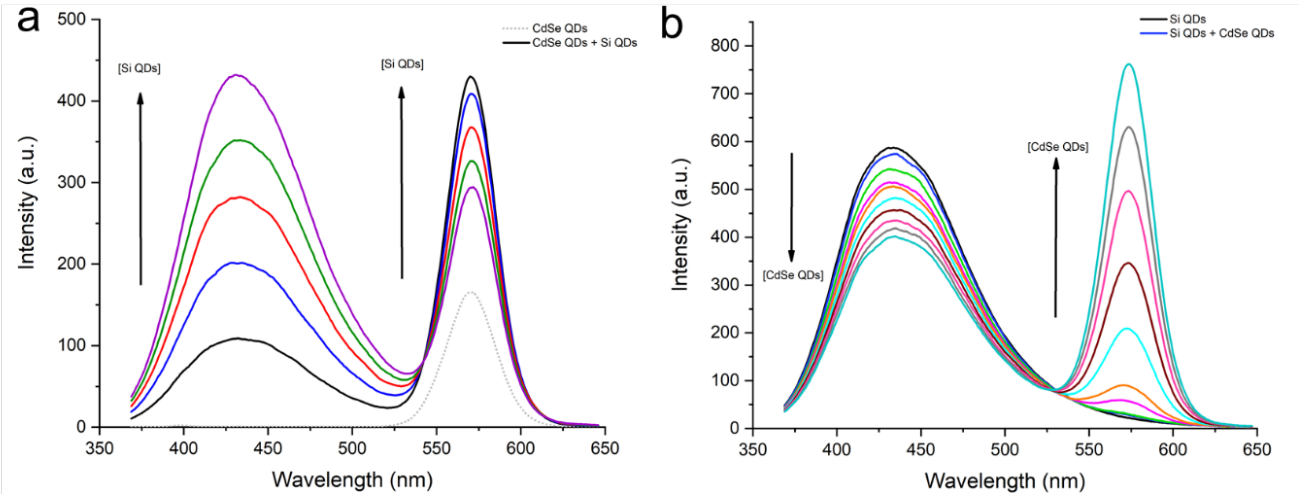

Figure S4. PL spectra of mixed QDs probe compared to those origin spectra.

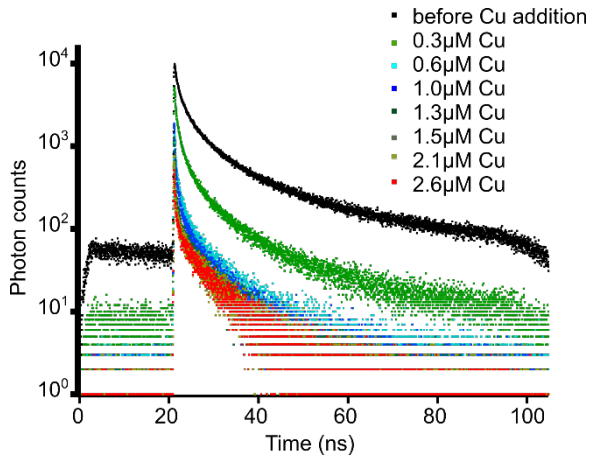

Figure S 5. Lifetime of CdSe QDs and Si QDs mixture before and after addition of Cu (probe at 575nm).

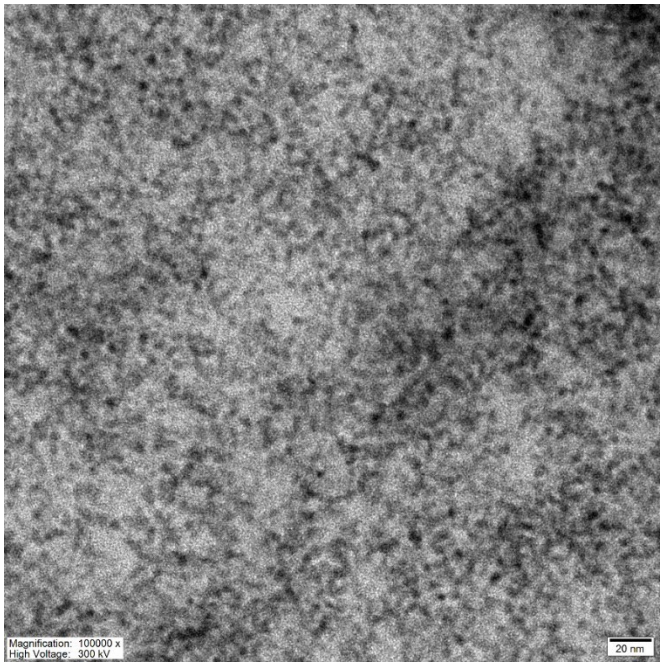

Figure S6. The FETEM image of the mixed-QDs probe.

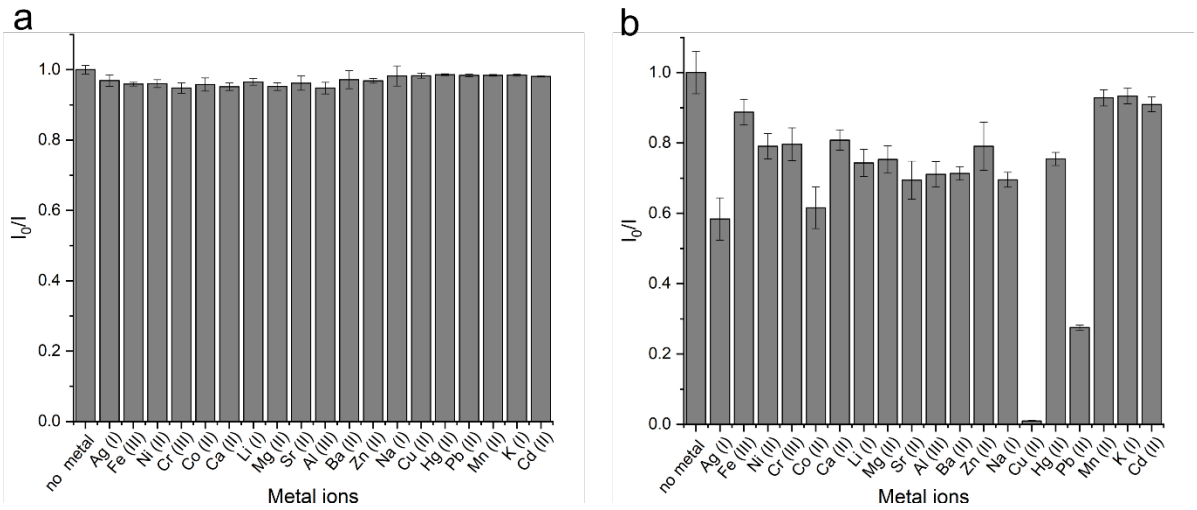

Figure S7. Effect of other cations on CdSe QD (a) and Si QDs (b).

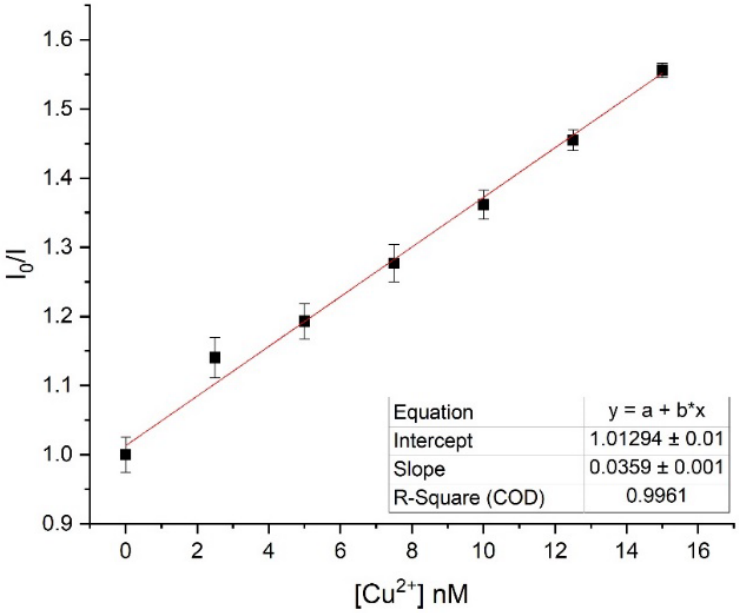

Figure S 8. Stern-Volmer's plot of CdSe QDs with Cu^{2+}

Table S 1. Amplitude average lifetime of Si QDs initially and after addition of CdSe QDs (probe at 485nm). Uncertainties in TR-PL parameters are 95% confidence intervals as reported by Horiba DeltaFlex software

	Si QDs initially	Si QDs+ 42uL CdSe QDs	Si QDs+ 84uL CdSe QDs	Si QDs+ 126uL CdSe QDs
τ avg (ns)	4.8±0.11	4.7±0.12	4.5±0.12	4.3±0.17
Chi Sq. (χ^2)	1.5	1.6	1.5	1.5

Table S 2. Amplitude average lifetime of CdSe QDs initially and after addition of CdSe QDs to Si QDs (probe at 575nm). Uncertainties in TR-PL parameters are 95% confidence intervals as reported by Horiba DeltaFlex software

	CdSe QDs	Si QDs + 42uL CdSe QDs	Si QDs + 84uL CdSe QDs	Si QDs + 126uL CdSe QDs
τ avg (ns)	1.0±0.12	1.8±0.24	4.1±0.29	4.1±0.32
Chi Sq. (χ^2)	1.9	1.3	2.8	2.3

Table S 3. Elemental analysis of Si QDs by FETEM

Element	Weight %	Atomic %
C	49.51	60.82
N	2.67	2.81
O	28.37	26.16
Si	19.45	10.21

Table S 4. Elemental analysis of CdSe QDs by FETEM

Element	Weight %	Atomic %
C	55.62	75.30
O	11.82	12.02
S	21.53	10.92
Cd	8.18	1.18
Se	2.84	0.59

Table S 5. Elemental analysis of mixed -QDs probe by FETEM

Element	Weight %	Atomic %
C	21.65	38.10
N	4.20	6.35
O	22.49	29.72
Si	23.81	17.93
S	5.46	3.60
Se	1.22	0.33
Cd	21.17	3.98